

Effect of sulfide ions on the stress corrosion behaviour of Al-brass and Cu10Ni alloys in salt water

S. M. SAYED, E. A. ASHOUR, G. I. YOUSSEF

Physical Chemistry Department, National Research Center, Dokki, Cairo, Egypt
E-mail: eaashour@Lycos.com

S. M. EL-RAGHY

Faculty of Engineering, Cairo University, Cairo, Egypt

The stress corrosion cracking (SCC) behavior of Al-brass and Cu10Ni alloys was investigated in 3.5% NaCl solution in absence and in presence of different concentrations of Na₂S under open-circuit potentials using the constant slow strain rate technique. The results indicated that the Cu10Ni alloy is more susceptible to stress corrosion cracking than as-received Al-brass at strain rate of $3.5 \times 10^{-6} \text{ s}^{-1}$ in 3.5% NaCl in presence of high concentration of sulfide ions (1000 ppm). The sulfide ions (up to 500 ppm) has no effect on the stress corrosion cracking of the annealed Al-brass in 3.5% NaCl at two strain rates of 7.4×10^{-6} and $3.5 \times 10^{-6} \text{ s}^{-1}$. The results support film rupture for Al-brass and sulfide stress corrosion cracking assisted with pitting corrosion for Cu10Ni at slip steps as the operating mechanisms. © 2002 Kluwer Academic Publishers

1. Introduction

Copper base alloys have a long history of service in marine environments and saline water systems, e.g. heat exchangers and distillation type desalination plants. Among the numerous Cu-base alloys Al-brass and Cu-Ni alloys are most frequently used in different chemical industries, multi-stage flash (MSF) in the desalination systems, water distribution systems and water treatment units. The corrosion resistance of copper alloys is often attributed to the formation of a protective corrosion product film on their surfaces [1–9]. During service these alloys are subjected to different stresses which in presence of corrosive environments sometimes lead to failure by stress corrosion cracking. Many of these failures were found to be due to the presence of some pollutants such as sulfide ions in seawater. These ions are known to promote the corrosion of copper and its alloys [10–16]. The stress corrosion cracking of Cu-Ni alloys had been investigated in seawater by Thompson [17] and in dilute, concentrated Na₂S solution at room temperature by Islam *et al.* [18]. The alloy was found to be susceptible to SCC under slow strain rate conditions in the concentrated (0.1 to 1 M) sulfide solution but it was not in the dilute solution (0.002 to 0.003 M). In another study [19] it was reported that the most severe SCC was observed on Cu30Ni in seawater with 3120 ppm sulfide ions at 25°C. El-Domiati and Alhajji [20] found that the SCC behaviour of CDA706 (Cu10Ni) is strictly linked to sulfide concentration in the range of 100 to 1000 ppm. Little work had been published on the SCC of Al-brass alloys. Todd [21] had reported that Al-brass tube failures in a desalina-

tion plant was due to severe intergranular corrosion attack which resulted from exposure to polluted seawater. Torchio and Mazza [22] had reported that chloride ions played a stimulating or an inhibitive role on the SCC of Al-brass in acidic sulfate solution depending upon their concentration, pH and copper ions content of the electrolyte.

The objective of the present work is to study and compare the susceptibility to SCC of modified Al-brass (MA 72) and Cu10Ni alloys in 3.5% NaCl and the role of the presence of different concentrations of Na₂S (100–1000 ppm) on the SCC behaviour of the two alloys.

2. Experimental procedure

The test materials were Al-brass (MA72) and Cu10Ni alloys which have the following chemical composition:

Al-brass (MA72): 71.62% Cu, 3.58% Al, 1.24% Ni, 0.034% Si, 0.038% Fe and the rest is Zn

Cu10Ni(CDA706): 88.12% Cu, 1.42% Fe, 0.38% Mn, 0.13% Zn, 0.01% Pb, and the rest is Ni

The mechanical properties of the two tested alloys are shown in Table I. A constant strain rate machine was used at a constant strain rates of 7.4×10^{-6} and $3.5 \times 10^{-6} \text{ s}^{-1}$ which were found to be the optimum values for studying the SCC of Cu-based alloys [18]. The specimens were machined to a gauge length of 25 mm and a diameter of 5 mm. They were polished with 320, 400 and 600 grade silicon carbide papers, degreased with acetone, rinsed with distilled water and coated with paraffin wax so that only the gauge length

TABLE I The mechanical properties of Al-brass and Cu10Ni alloys

| Alloys | Ultimate tensile stress (UTS), MPa | Yield strength (YS), MPa | Elongation % |
|----------------------|------------------------------------|--------------------------|--------------|
| As-received Al-brass | 504 | 500 | 18.28 |
| Annealed Al-brass | 495 | 330 | 20.3 |
| As-received Cu10Ni | 366.7 | 180 | 28 |

was exposed to the test solution. Some of the specimens which were prepared from the as-received Al-brass (MA72) were annealed for 6 hours at 400°C. The experiments were carried out at $24 \pm 1^\circ\text{C}$ in air and in aerated 3.5% NaCl in absence and in presence of different concentrations of Na₂S (100–1000 ppm). The cell used was a 200 ml glass cylinder, closed by upper and lower stoppers, through which the ends of the specimen protruded. Cracked specimens were removed from the solution after failure, cut 1 cm beyond the crack tip, and subjected to investigation by both optical and scanning electron microscopy (SEM) using JSM-T 20, JEOL, Japan.

3. Results and discussion

3.1. The SCC measurements of Al-brass

The stress-strain curves for the as-received Al-brass and annealed Al-brass in 3.5% NaCl solution in absence and in presence of different concentrations of Na₂S at strain rates $7.4 \times 10^{-6} \text{ s}^{-1}$ and $3.5 \times 10^{-6} \text{ s}^{-1}$ are shown in Figs 1–4. The curves have the same general

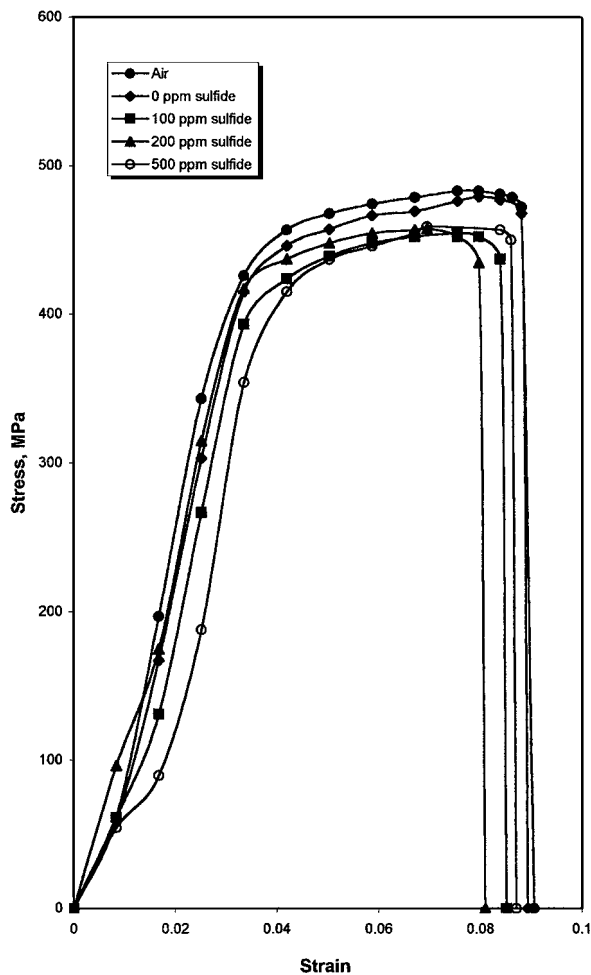


Figure 1 Stress-strain curves of as-received Al-brass in 3.5% NaCl solutions in absence and in presence of different concentrations of Na₂S at strain rate of $7.4 \times 10^{-6} \text{ s}^{-1}$.

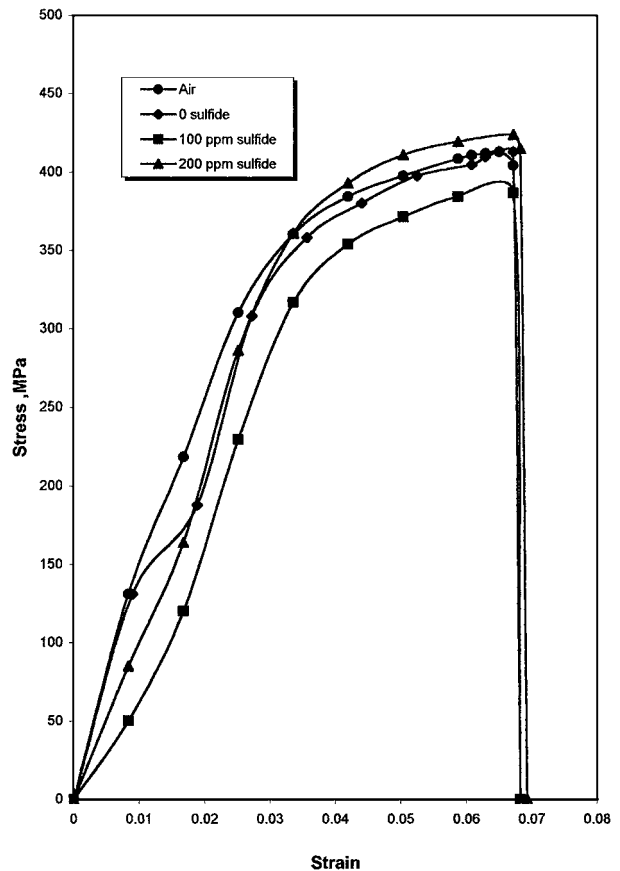


Figure 2 Stress-strain curves of annealed Al-brass in 3.5% NaCl solutions in absence and in presence of different concentrations of Na₂S at strain rate of $7.4 \times 10^{-6} \text{ s}^{-1}$.

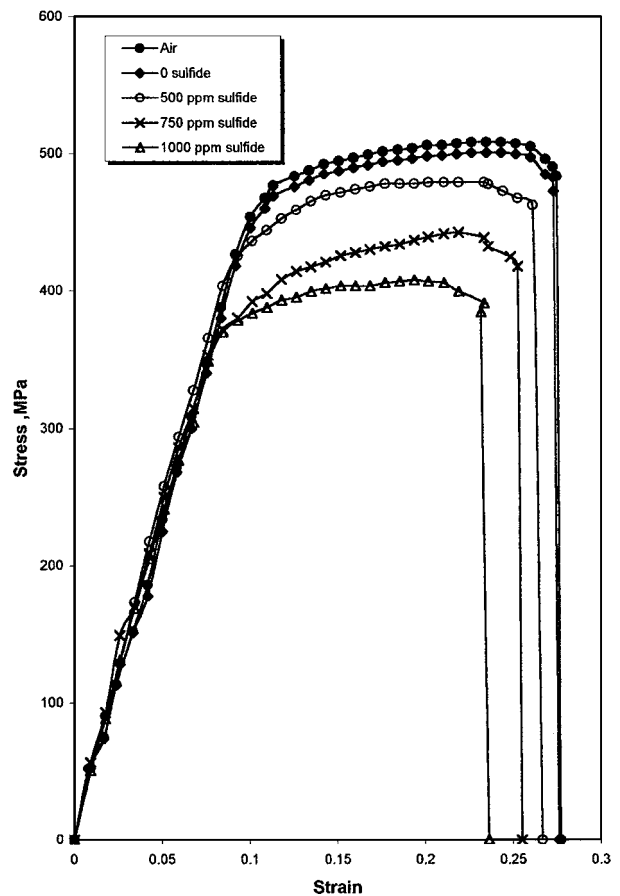


Figure 3 Stress-strain curves of as-received Al-brass in 3.5% NaCl solutions in absence and in presence of different concentrations of Na₂S at strain rate of $3.5 \times 10^{-6} \text{ s}^{-1}$.

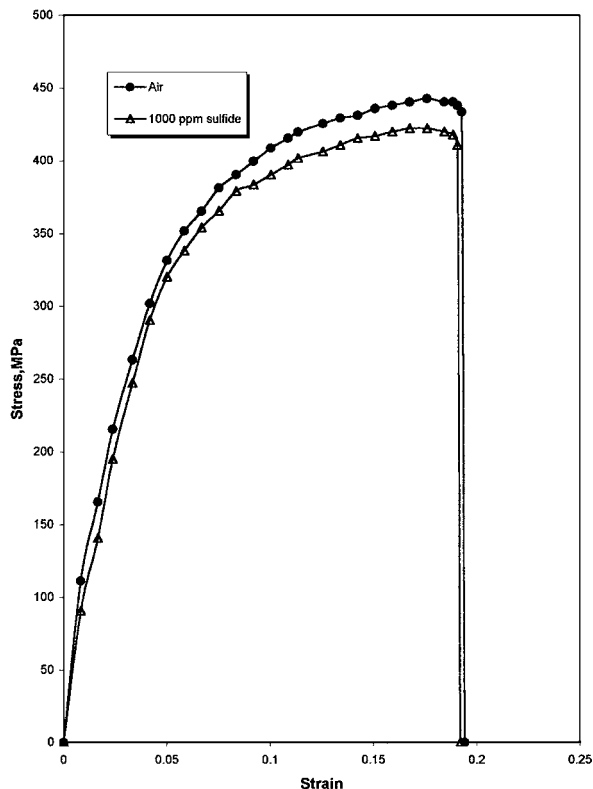


Figure 4 Stress-strain curves of annealed Al-brass in 3.5% NaCl solutions in absence and in presence of different concentrations of Na_2S at strain rate of $3.5 \times 10^{-6} \text{ s}^{-1}$.

shape and characterized by an initial rapid increase of stress with increasing strain up to the yield stress followed by a slight gradual increase in the form of plateau to reach a maximum after which the stress begins to decline to reach the point of failure. The curves of Figs 1 and 2 show very small differences and almost identical to the curves in air and in pure 3.5% NaCl solution (0 ppm S^{2-}). In order to make the role of the chemical factor (corrosion) more obvious, the applied strain rate was reduced to $3.5 \times 10^{-6} \text{ s}^{-1}$. The curves obtained are shown in Figs 3 and 4. The curves of Fig. 3 show that the increase of sulfide concentration considerably reduces both the maximum stress and time to failure i.e. increase the susceptibility of the as-received alloy to SCC under test conditions. On the other hand, the curves of Fig. 4 indicate that the annealed Al-brass is not susceptible to SCC under the test condition up to 1000 ppm sulfide. The susceptibility of stress corrosion was measured by the ratios of both the maximum stress (r) and the time to failure (τ).

$$r = \sigma_{\max}(\text{sol.})/\sigma_{\max}(\text{air}) \quad (1)$$

$$\tau = t_f(\text{sol.})/t_f(\text{air}) \quad (2)$$

Where σ_{\max} = maximum tensile stress, t_f = time to failure, both r and τ were combined in a quantitative phenomenological expression for the susceptibility (s) to SCC as follows [23]:

$$S = [(1 - r)(1 - \tau)]^{1/2} \quad (3)$$

The value of toughness (U (MJ/m^3)) is also a useful criteria for assessing susceptibility to SCC which is defined as the area under the curve of stress-strain.

TABLE II Effect of sulfide concentration on the SCC parameters for as-received and annealed Al-brass in 3.5% NaCl at strain rate of $7.4 \times 10^{-6} \text{ s}^{-1}$ (see text)

| Sulfide conc. (ppm) | As-received Al-brass | | | | | Annealed Al-brass | | | | |
|---------------------|----------------------|--------|-------|-------|-------|-------------------|--------|-----|-------|-------|
| | r | τ | s | u | U^* | r | τ | S | u | U^* |
| 0 | 0.99 | 0.90 | 0.014 | 40.27 | 0.98 | 1 | 1 | - | 25.67 | 0.97 |
| 100 | 0.94 | 0.94 | 0.06 | 36.97 | 0.90 | 0.94 | 1 | - | 24.48 | 0.93 |
| 200 | 0.95 | 0.90 | 0.07 | 35.72 | 0.87 | 1.02 | 1.01 | - | 27.42 | 1.04 |
| 500 | 0.95 | 0.97 | 0.038 | 38.06 | 0.93 | - | - | - | - | - |

TABLE III Effect of sulfide concentration on the SCC parameters for as-received Al-brass and Cu10Ni in 3.5% NaCl at strain rate of $3.5 \times 10^{-6} \text{ s}^{-1}$

| Sulfide conc. (ppm) | Cu10Ni | | | | | As-received Al-brass | | | | |
|---------------------|--------|--------|-------|------|-------|----------------------|--------|-------|-------|-------|
| | r | τ | s | U | U^* | r | τ | s | U | U^* |
| 0 | 0.99 | 0.98 | 0.014 | 56.2 | 0.98 | 0.98 | 0.99 | 0.014 | 129 | 0.98 |
| 500 | 0.94 | 0.90 | 0.077 | 49 | 0.85 | 0.94 | 0.96 | 0.048 | 118.8 | 0.89 |
| 750 | 0.90 | 0.79 | 0.144 | 39.8 | 0.69 | 0.89 | 0.92 | 0.093 | 105.5 | 0.79 |
| 1000 | 0.83 | 0.70 | 0.225 | 27 | 0.47 | 0.80 | 0.85 | 0.173 | 94.18 | 0.71 |

$$\text{The ratio of toughness}(U^*) = U(\text{sol.})/U(\text{air}) \quad (4)$$

Table II summarizes the above SCC parameters of as-received and annealed Al-brass in 3.5% NaCl solutions with different concentrations of sulfide ions at strain rate of $7.4 \times 10^{-6} \text{ s}^{-1}$. Also, the results of as-received Al-brass in the same test solutions at strain rate of $3.5 \times 10^{-6} \text{ s}^{-1}$ are shown in Table III.

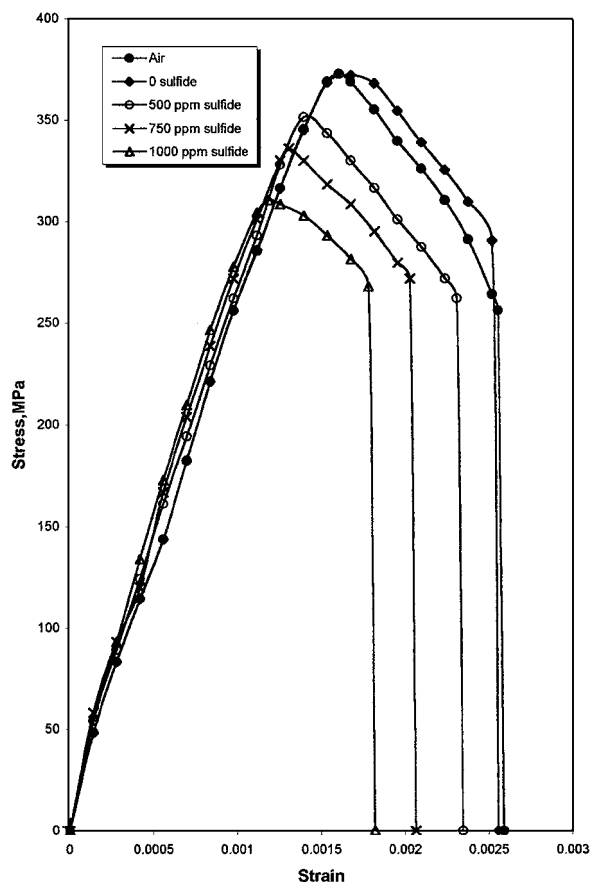


Figure 5 Stress-strain curves of Cu10Ni in 3.5% NaCl solutions in absence and in presence of different concentrations of Na_2S at strain rate of $3.5 \times 10^{-6} \text{ s}^{-1}$.

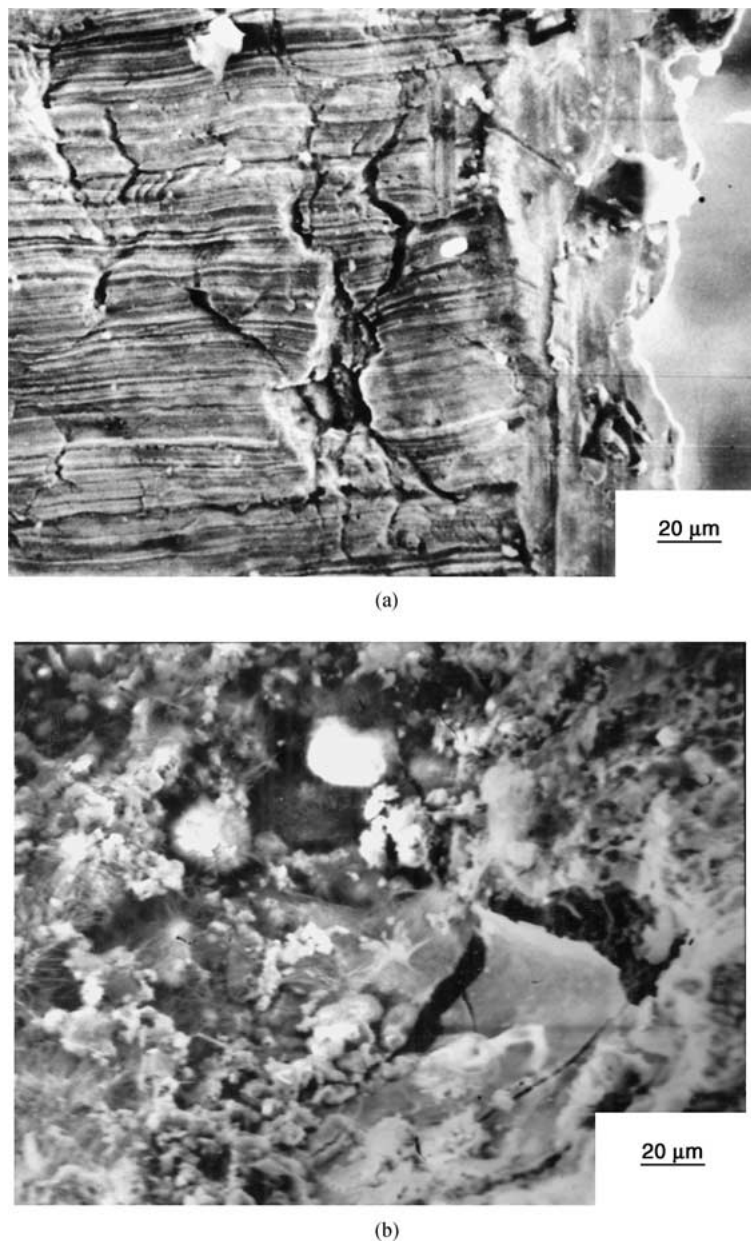


Figure 6 SEM fractograph of the SCC for Al-brass in 3.5% NaCl + 1000 ppm sulfide ions (a) fracture surface, (b) exposed surface.

3.2. SCC measurements of Cu10Ni alloy

Fig. 5 shows the stress-strain curves of Cu10Ni in 3.5% NaCl in absence and in presence of different concentrations of Na₂S at strain rate of $3.5 \times 10^{-6} \text{ s}^{-1}$. The curves have the same general shape which is characterized by a rapid linear increase of stress with increasing strain to the point of maximum stress and decrease gradually to reach the point of failure. The effect of increasing of sulfide ions concentrations (≥ 500 ppm) reveals a considerable reduction in the maximum stress, toughness as well as the time of failure. The results are summarized in Table III. It is clear from Figs 3 and 5 that Al-brass has a wide range of plastic deformation than that of Cu10Ni.

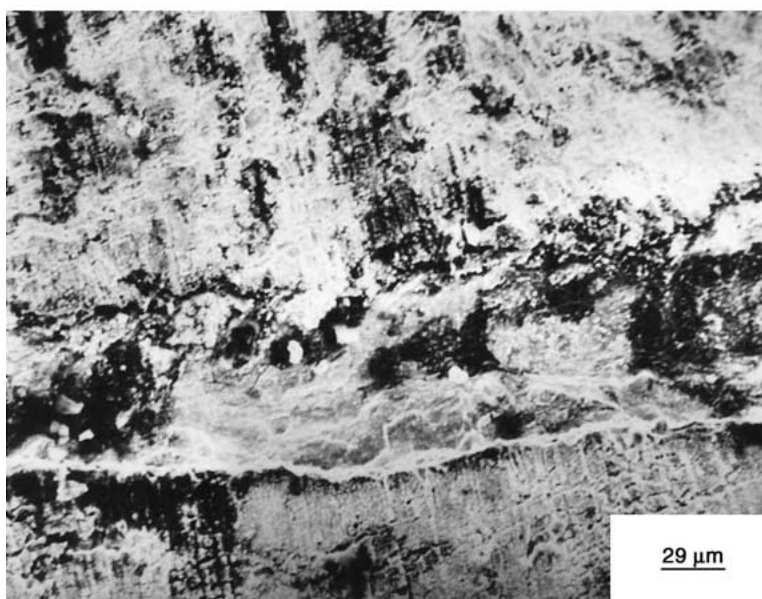
3.3. Metallographic investigations of Al-brass and Cu10Ni

Metallographic investigations are always used to verify the occurrence of SCC in the failed specimens. The

SEM micrographs of Figs 6 and 7 show the fracture and exposed surfaces of Al-brass and Cu10Ni failed by the slow strain rate tests in 3.5% NaCl solutions in presence of 1000 ppm sulfide ions. The metallographic appearance of the fracture surfaces in most tests in solutions containing sulfide less than 500 ppm displayed ductile failure similar to that occurred in air. It is obvious at concentration 1000 ppm Na₂S that the secondary cracks become more intense and spreads along a wide range of the specimen surfaces for Al-brass and Cu10Ni as shown in Figs 6b and 7b, respectively. The fracture mode of Al-brass was mixed mode (intergranular(IG) + transgranular(TG)) with the presence of intensive secondary microcracks at the exposed surface. Also, the fracture mode of Cu10Ni was mixed mode but predominantly intergranular. There was intergranular secondary microcracks at the exposed surface of Cu10Ni but not in the same intensity as that of Al-brass. From the above we can suggest that the mechanism of stress corrosion cracking of Al-brass in NaCl solution



(a)



(b)

Figure 7 SEM fractograph of the SCC for Cu10Ni in 3.5% NaCl + 1000 ppm sulfide ions (a) fracture surface, (b) exposed surface.

containing high concentrations of Na_2S is the film rupture according to the thin adhesive nature of film formed (mainly Cu_2O). The intensive microcracks formed near the crack tip on the exposed surface which supplies in presence of stress a new bare surface to be attacked by the solution and allows the crack to propagate. The suggested mechanism for Cu10Ni in the same solutions and strain rate is sulfide induced cracking or sulfide stress corrosion cracking according to the nature of the film formed of Cu_2S and Cu_2O which was thick, brittle, porous and less adherent. In this case, it is more easier under the influence of tensile stress to initiate cracking from the corrosion pits and allow its propagation. It was found that a synergism exists between sulfide and stress that enhances the latter [20].

4. Conclusions

1. The sulfide ions (up to 500 ppm) has no effect on the stress corrosion cracking of the annealed Al-brass

in 3.5% NaCl at two strain rates of $7.4 \times 10^{-6} \text{ s}^{-1}$ and $3.5 \times 10^{-6} \text{ s}^{-1}$.

2. Cu10Ni alloy is more susceptible to SCC than as-received Al-brass at strain rate of $3.5 \times 10^{-6} \text{ s}^{-1}$ in presence of high concentrations of sulfide ions (1000 ppm).

3. The fracture mode of as-received Al-brass was mixed mode (IG + TG cracking) with the presence of intensive secondary microcracks at the exposed surface.

4. The fracture mode of Cu10Ni was mixed mode (IG + TG) but predominantly intergranular with secondary microcracks at the exposed surface.

5. The results support the film rupture for Al-brass and sulfide stress corrosion cracking assisted with pitting corrosion for Cu10Ni as the operating mechanisms.

References

1. A. H. TUTHILL, *Materials Performance* **26** (1987) 12.
2. R. F. NORTH and M. J. PRYOR, *Corros. Sci.* **10** (1970) 197.

3. B. G. ATEYA, E. A. ASHOUR and S. M. SAYED, *J. Electrochem. Soc.* **141** (1994) 71.
4. B. LITTLE and F. MANSFELD, *Werk. und Korros.* **42** (1991) 331.
5. H. J. MUELLER, *Corrosion* **45** (1989) 735.
6. H. W. HOPPE and H. H. STREHBLOW, *Corros. Sci.* **31** (1990) 167.
7. E. A. ASHOUR and B. G. ATEYA, *ibid.* **37** (1995) 371.
8. R. N. SINGH, N. VERMA and W. R. SINGH, *Corrosion* **35** (1989) 222.
9. J. CROUSIER and J. P. CROUSIER, *ibid.* **44** (1988) 768.
10. D. D. MACDONALD, B. C. SYRETT and S. S. WING, *ibid.* **35** (1979) 409.
11. C. KATO, H. W. PICKERING and J. E. CASTLE, *J. Electrochem. Soc.* **131** (1984) 1225.
12. J. P. GUDAS and H. P. HACK, *Corrosion* **35** (1979) 67.
13. H. M. SHALABY, A. AL-HASHEM and K. AL-MUHANNA, *Brit. Corros. J.* **31** (1996) 199.
14. S. JACOBS and M. EDWARDS, *Water Research* **34** (2000) 2798.
15. J. N. ALHAJJI and M. R. REDA, *J. Electrochem. Soc.* **142** (1995) 2944.
16. E. A. ASHOUR, *J. Mater. Sci.* **36** (2000) 201.
17. D. THOMPSON, *Material Research Study* **1** (1961) 108.
18. M. ISLAM, W. T. RAID, S. AL-KHARRAZ and S. ADO-NAMOUS, *Corrosion* **47** (1991) 4.
19. K. HABIB and A. HUSAIN, *Desalination* **97** (1994) 29.
20. A. EL-DOMIATY and J. N. ALHAJJI, *J. Materials Engineering and Performance* **6** (1997) 534.
21. B. TODD, *Desalination* **3** (1967) 106.
22. S. TORCHI and F. MAZZA, *Corros. Sci.* **26** (1984) 813.
23. E. A. ASHOUR, E. A. ABD EL-MEGUID and B. G. ATEYA, *Corrosion* **53** (1997) 612.

*Received 23 July 2001
and accepted 30 January 2002*